SAFE WAVE

STREAMLINING THE ASSESSMENT OF ENVIRONMENTAL EFFECTS OF WAVE ENERGY

DELIVERABLE 3.3
Marine Dynamic Modelling

Co-funded by the EMFF programme of the European Union

WP 3

Deliverable 3.3 Marine Dynamics Modelling

Lead partner for deliverable:

AZTI

AUTHORS

Iñaki de Santiago (AZTI)
Pedro Liria (AZTI)
Roland Garnier (AZTI)
Juan Bald (AZTI)
José Chambel Leitão (Hidromod)
João Ribeiro (Hidromod)

SUBMISSION DATE

21| June| 2023

DISSEMINATION LEVEL

PU	Public	X
CL	Classified – EU classified (EU-CONF, EU-RESTR, EU-SEC) under Commission Decision No 2015/444	
CO	Confidential, only for members of the consortium (including Commission Services)	

DOCUMENT HISTORY

Issue Date	Version	Changes Made / Reason for this Issue
June 21, 2023	1	

CITATION

Santiago, I., Liria, P., Garnier, R., Bald, J., Leitão, J.C., Ribeiro, J., 2023. Deliverable 3.3 Marine dynamics modelling. Corporate deliverable of the SafeWAVE Project co-funded by the European Climate, Infrastructure and Environment Executive Agency (CINEA), Call for Proposals EMFF-2019-1.2.1.1 - Environmental monitoring of ocean energy devices. DOI: http://dx.doi.org/10.13140/RG.2.2.36716.74886. 35 pp + Annexes.

This communication reflects only the author´s view. CINEA is not responsible for any use that may be made of the information it contains.

This Project is co-funded by the European Climate, Infrastructure and Environment Executive Agency (CINEA), Call for Proposals EMFF-2019-1.2.1.1 - Environmental monitoring of ocean energy devices.

CONTENTS

1. SAFE WAVE project synopsis

The European Atlantic Ocean offers a high potential for marine renewable energy (MRE), which is targeted to be at least 32% of the EU's gross final consumption by 2030 (European Commission, 2020 (European Commission, 2020). The European Commission is supporting the development of the ocean energy sector through an array of activities and policies: the Green Deal, the Energy Union, the Strategic Energy Technology Plan (SET-Plan) and the Sustainable Blue Economy Strategy. As part of the Green Deal, the Commission adopted the EU Offshore Renewable Energy Strategy (European Commission, 2020) which estimates to have an installed capacity of at least 60 GW of offshore wind and at least 1 GW of ocean energy by 2030, reaching 300 GW and 40 GW of installed capacity, respectively, moving the EU towards climate neutrality by 2050.

Another important policy initiative is the REPowerEU plan (European Commission, 2022) which the European Commission launched in response to Russia's invasion of Ukraine. REPowerEU plan aims to reduce the European dependence amongst Member States on Russian energy sources, substituting fossil fuels by accelerating Europe's clean energy transition to a more resilient energy system and a true Energy Union. In this context, higher renewable energy targets and additional investment, as well as introducing mechanisms to shorten and simplify the consenting processes (i.e., 'go-to' areas or suitable areas designated by a Member State for renewable energy production) will enable the EU to fully meet the REPowerEU objectives.

The nascent status of the Marine Renewable Energy (MRE) sector and Wave Energy (WE) in particular, yields many unknowns about its potential environmental pressures and impacts, some of them still far from being completely understood. Wave Energy Converters' (WECs) operation in the marine environment is still perceived by regulators and stakeholders as a risky activity, particularly for some groups of species and habitats.

The complexity of MRE licensing processes is also indicated as one of the main barriers to the sector development. The lack of clarity of procedures (arising from the lack of specific laws for this type of projects), the varied number of authorities to be consulted and the early stage of Marine Spatial Planning (MSP) implementation are examples of the issues identified to delay projects' permitting.

Finally, there is also a need to provide more information on the sector not only to regulators, developers and other stakeholders but also to the general public. Information should be provided focusing on the ocean energy sector technical aspects, effects on the marine environment, role on local and regional socio-economic aspects and effects in a global scale as a sector producing clean energy and thus having a role in contributing to decarbonise human activities. Only with an informed society would be possible to carry out fruitful public debates on MRE implementation at the local level.

These non-technological barriers that could hinder the future development of WE in EU, were addressed by the WESE project funded by European Maritime and Fisheries Fund (EMFF) in 2018. The present project builds on the results of the WESE project and aims to move forward through the following specific objectives:

1. Development of an **Environmental Research Demonstration Strategy** based on the collection, processing, modelling, analysis and sharing of environmental data collected in WE sites from different European countries where WECs are currently operating (Mutriku power plant and BIMEP in Spain, Aguçadoura in Portugal and SEMREV in France); the SafeWAVE project aims to enhance the understanding of the negative, positive and negligible effects of WE projects. The SafeWAVE project will continue previous work, carried out under the WESE project, to increase the knowledge on priority research areas, enlarging the analysis to other types of sites, technologies and countries. This will increase information robustness to better inform decision-makers and managers on real environmental risks, broaden the engagement with relevant stakeholders, related sectors and the public at large and reduce environmental uncertainties in consenting of WE deployments across Europe;
2. Development of a **Consenting and Planning Strategy** through providing guidance to ocean energy developers and to public authorities tasked with consenting and licensing of WE projects in France and Ireland; this strategy will build on country-specific licensing guidance and on the application of the MSP decision support

tools (i.e. WEC-ERA[1] by Galparsoro et al., 2021[2] and VAPEM[3] tools) developed for Spain and Portugal in the framework of the WESE project; the results will complete guidance to ocean energy developers and public authorities for most of the EU countries in the Atlantic Arch.

3. Development of a **Public Education and Engagement Strategy** to work collaboratively with coastal communities in France, Ireland, Portugal and Spain, to co-develop and demonstrate a framework for education and public engagement (EPE) of MRE enhancing ocean literacy and improving the quality of public debates.

[1] https://aztidata.es/wec-era/;
[2] Galparsoro, I., M. Korta, I. Subirana, Á. Borja, I. Menchaca, O. Solaun, I. Muxika, G. Iglesias, J. Bald, 2021. A new framework and tool for ecological risk assessment of wave energy converters projects. Renewable and Sustainable Energy Reviews, 151: 111539
[3] https://aztidata.es/vapem/

2. Executive summary

The current global situation, in a climate change context, urges to find new ways to capture energy with low greenhouse gas emissions. In this sense, ocean energy can positively contribute to the reduction of greenhouse gas emissions by producing clean energy.

The main purpose of the work is to; i) validate the current wave propagation model at BIMEP zone (northern Spain, Basque Coast) and ii) to test and/or consolidate different downscaling strategies for this kind of studies. On the other hand, in the Aguçadoura test site, located in the northern region of Portugal, the aim is to study the influence of an array of WECs on coastal processes, mainly sediment transport at the beach.

The model grid cell size sensitivity test shows that there is a clear relationship between the grid cell size and the computational cost. However, the grid cell sizes tested in the present work have a limited impact on the output highlighting the model robustness and stability. On the other hand, the comparison between Downscaling methods reveals the suitability of Hybrid Statistical Downscaling approach to be carried out in probabilistic wave farm coastal impact studies. The differences between the use of Dynamic Downscaling and Hybrid Statistical Downscaling are small and acceptable for this type of work (RMSE is below 0.28m, 1.52s and 13.14º for Hs, Tp and θp).

For the Aguçadoura test site in Portugal, there is a 68% reduction in energy to the lee of the equipment over a 15-day period. The shadowing effect gradually diminishes towards the shore, with the reduction nearshore being less than 2%. The WEC farm located at the Aguçadoura site would not influence the sediment transport at the shore or any other processes.

Finally, it is essential to consider the computational effort needed to simulate the WEC farm. To accurately assess the extent of the wave farm's influence, large computational domains are required. Additionally, the computational grid must have a resolution capable of simulating the WEC unit. These two factors make the simulation effort very time-consuming and for these reasons other approaches should be tested. The options may vary from using other models similar to SNL-SWAN, or even adopting a statistical downscaling approach following the methodology described for the BIMEP case.

3. Introduction

The current global situation, in a climate change context, urges to find new ways to capture energy with low greenhouse gas emissions. In this sense, ocean energy can positively contribute to the reduction of greenhouse gas emissions by producing clean energy.

Although in recent years the wave energy extraction technology is growing fast, their effects on coastal environments must be well studied as the removal of part of this energy can lead to hydrodynamic changes that may affect the coastal zone (e.g. change in current patterns, sediment transport rates).

In previous studies related to BIMEP (de Santiago, I., Moura, T., Chambel, J., Liria, P., and Bald, 2020), the characterization of the coastal zone impact was carried out. This was analysed through the impact of wave energy removal at the coastal zone and the sediment transport impact on beaches through a Statistical Hybrid Downscaling approach.

In the present study, the validation of the methodology followed in the WESE project (https://wese-project.weebly.com/) is carried out. To this end, '*in situ*' wave parameter measures are compared with modelled data followed in the WESE approach. The main purpose of the work is to; i) validate the current wave propagation model at BIMEP zone and ii) to test and/or consolidate different downscaling strategies for this kind of studies.

In the Aguçadoura test site, located in the northern region of Portugal, the aim is to study the influence of an array of WECs on coastal processes, mainly sediment transport at the beach. This document describes a set of simulations carried out using the SNL-SWAN model for a farm of WEC units, specifically focusing on the HiWave-5 point absorber developed by CorPower Ocean. To accurately model the WEC units, Hidromod utilized a power matrix provided by CorPower and input spectral wave energy boundary conditions that represented high-energy events over a 15-day period. The simulations employed a spectral boundary condition from Hidromod's operational wave model for the Portuguese coast, which is validated daily using wave parameters from Instituto Hidrográfico's buoys.

4. BIMEP

4.1 Study site

The BIMEP zone (Figure 1) provides an area for offshore research, test, demonstration, and validation of wave energy generation devices. It is located in the Basque coast (northern Spain) within the Bay of Biscay. The BIMEP zone covers an area of 5.3 km^2, lies at a depth of 50 – 90 m and is 1.8-4.5 km far from the coast.

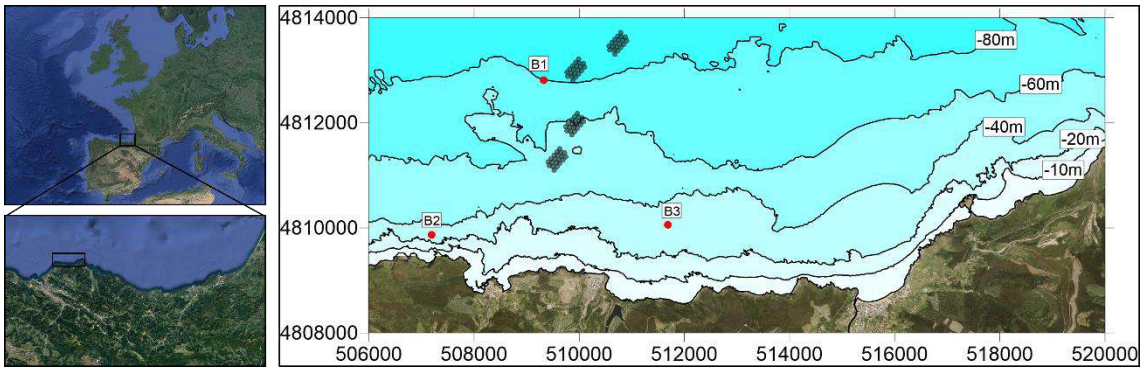

Figure 1 - Case study location (BIMEP zone, Basque Coast, Spain, Europe). Black dots: WEC devices. Red dots: Wave buoys.

The wave climate in the Basque coast is characterized by energetic and seasonally variable wave climate. The mean offshore significant wave height (Hs), peak period (Tp) and wave peak direction (θ_p) is 1.5m, 10s and 350°, respectively. The tidal regime of the region is semi-diurnal and it is classified as low-mesotidal during neap tides, and high-mesotidal during spring tides presenting a maximum annual tidal range that exceeds 4.5m.

4.2 Material and methods

4.2.1 Hydrodynamic conditions

4.2.1.1 Offshore wave data

The wave data was collected from the Downscaling Ocean Waves (DOW) database (Camus et al., 2013) and the offshore wave data was collected from the Bilbao Vizcaya wave buoy (Puertos del Estado). The Dow dataset is composed by 61 years of hourly spaced coastal waves. The Bilbao Vizcaya wave buoy is deployed offshore at deep waters (590 m water depth) and is composed by 33 years (since 1990) of hourly spaced offshore waves.

4.2.1.2 Bimep wave data

The validation of the nearshore wave propagation model was carried out at the three different locations (Figure 1):

B1) Bimep buoy: 80m

The buoy is moored 4 km off the coast of Armintza in approximately 80 m water depth. It processes and transmits the main wave parameters in an hourly basis but also stores the rough data of pitch, roll, heave and compass (2048 data every hour with a frequency of 2 Hz). The buoy is also equipped with meteorological sensors, an electromagnetic current sensor (2 m below the surface) and an Acoustic Current Profiler (RDI 600 MHz) which measures the current velocity profile from 11 m to the sea floor (2 m cells).

B2) and B3) Two acoustic doppler wave and current profiler Nortek AWAK-1MHz were installed in approximately 30 m depths to measure waves simultaneously. Two different points were selected, one to the west of Armintza and out of the possible area of influence of the wave shadow effects of BIMEP and another one directly in the lee of BIMEP shadowing effects. The instruments were identically configured and measured hourly wave directional parameters from 01/18/2012 to 02/25/2012, previously to the installation of marine energy devices in BIMEP.

4.2.1.3 Water level

The water level information is obtained from the Bilbao3 tidal gauge. It is located 1070 metres offshore of Santurtzi shore. The dataset is composed by 31 years (since 1992) and stores the water level at 1 minute time intervals.

4.2.2 Wave model

The model tested in the present study is the SNL-SWAN (Chang et al., 2016). The model was originally created to evaluate the WEC farm effects on wave propagation. The model incorporates a WEC module that internally calculates the transmission coefficients based on the WEC power performance. If the WEC module is turned off the model acts as a SWAN model (Booij et al., 1999) It is a wave energy propagation spectral model. The model simulates wave generation, propagation and dissipation including the effects of wave refraction and reflection. It also accounts for wave

dissipation by white-capping processes, bottom friction and wave breaking. The model is suitable for wave propagation on a regional scale ($O(10^3)$ km).

4.2.3 Wave downscaling methods

Downscaling is the procedure of inferring high resolution information from low resolution variables. In the case of the wave climate downscalling, the process is carried out by nesting wave propagation models. Depending on the type of model (e.g. processes solved, numerical scheme used), the temporal extent (e.g. number of sea states) and the area to be analysed (e.g. extent of grids and spatial discretisation), the computational cost can vary considerably. There are three different downscaling methods:

a) Dynamical downscaling: It consists of nesting a wave propagation model from deep water to shallow water solving all the processes involved (refraction, bottom friction, shoaling, diffraction, breaking). It allows to dynamically infer the effects of large-scale processes to regional or local scales.

b) Statistical downscaling: It consists of empirical relationship between deep water wave climate parameters and nearshore wave climate parameters.

c) Hybrid Statistical downscaling: It combines dynamical downscaling and statistical downscaling in order to reduce the computational effort (Camus et al., 2011).

In the present case the Dynamic Downscaling is compared against a Hybrid Statistical Downscaling.

For the Hybrid Statistical Downscaling, a three-step approach is used:

1. The maximum dissimilarity selection algorithm (MDA) is applied to obtain a representative sea state dataset. In the present case, 350 sea states were selected from the DOW dataset (Figure 2).
2. Each sea state is propagated to the coastal area.
3. Once the sea states are propagated to the coast, the wave parameters (wave height, wave period, wave direction) are reconstructed using a non-linear interpolation technique based on radial basis functions (RBFs), at B1, B2 and B3 locations (see Figure 1).

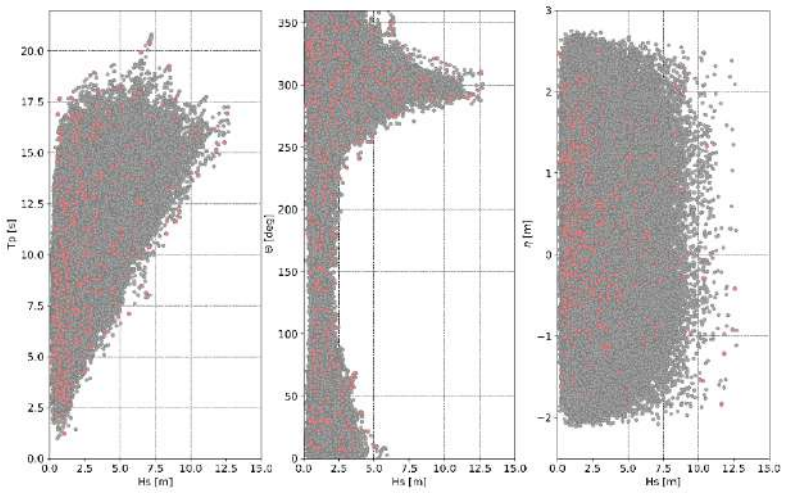

Figure 2 - Wave climate parameters distribution at the Bilbao Vizcaya buoy (lat=43.64° lon=-3.09°). Grey dots: all sea states of DOW dataset at the Bilbao Vizcaya buoy. Red dots: Selected cases for wave propagation using the MDA algorithm.

4.3 Results

4.3.1 Sensitivity of model results related to the mesh size

A series of grid cell size (dx, dy) sensitivity tests were conducted. For that, three grid configurations were tested; i) fine grid (taken as reference), ii) medium grid, iii) coarse grid. Results are compared at six control locations (control points) along the nearshore area of the Basque coast. For each numerical grid configuration (Table 1), 45 sea states were propagated. These sea states were obtained by combining three significant wave heights (Hs = 1m ,3m ,8 m), three peak periods (Tp = 6s, 14s, 20s) and four main wave propagation directions (θ_p = 292.5°, 315°, 337.5°, 360°, 22.5°). All sea states were propagated using a Jonswap spectrum, assuming a frequency dispersion parameter (γ) of 3.3 and a directional dispersion of 20°.

The diagnostic statistics used to obtain the model performance are the computational cost and the root mean square error (RMSE). C1 grid configuration is used as the reference scenario. There is a clear relationship between the grid cell size and the computational cost. C3 and C2 configurations take 4.5 and 1.5 times longer than C1, respectively. The grid cell sizes tested in the present work have a limited impact on the output (Figure 3). In general, C3 grid configuration has larger error than C2. The model accuracy drops with large input values of Hs, Tp and wave incidence angle. However, the maximum RMSE values for C3 are 0.5 m, 0.4 s and 2° for Hs, Tp and θp, respectively.

Table 1. Model grid configurations.

Configuration	Mesh name/domain	Cell Size [m]
C1	Regional (120km x 40 km)	500
	Sub-regional (61Km x 23Km)	100
	Detail (8km x 4 km)	25
C2	Regional (120km x 40 km)	700
	Sub-regional (61Km x 23Km)	140
	Detail (8km x 4 km)	35
C3	Regional (120km x 40 km)	1000
	Sub-regional (61Km x 23Km)	250
	Detail (8km x 4 km)	50

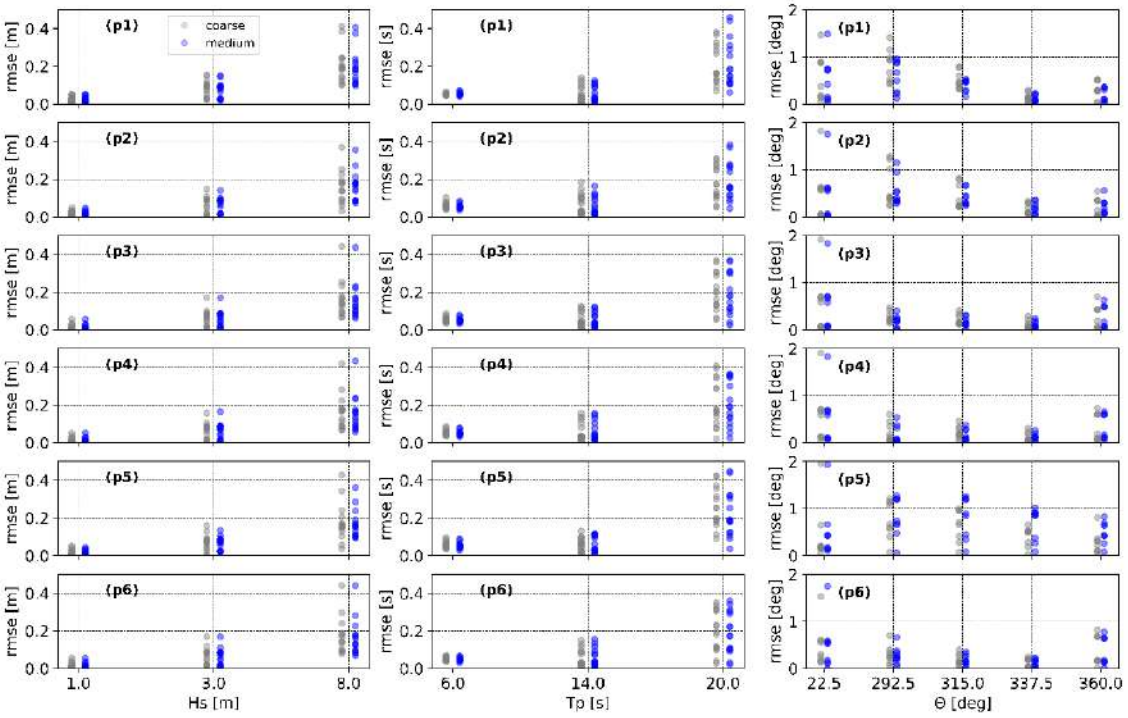

Figure 3 – Comparison of model grid configuration as function of wave input parameters.

4.3.2 Downscaling method validation

The validation of the propagated wave time series was compared against measured data at B1, B2 and B3 locations (Figure 1). The comparison was made during variable

wave conditions (Hs ranging from 4.9m to 0.4m, respectively). Both, Hs, Tp and θp were available for comparison. Both the Hybrid Statistical and Dynamic Downscaling methods were tested. The Dynamic Downscaling was only performed for the period where the wave buoy data was available, and it is only used for comparison purposes. The diagnostic statistics used to obtain the model performance are the root mean square error (RMSE), the Pearson's correlation coefficient (ρ), the systematic deviation between two random variables (BIAS), the residual scatter index (SI) and the standard deviation (std).

The results are resumed in Figure 4. The RMSE is below 0.28m, 1.52s and 13.14° for Hs, Tp and θp, respectively and the correlation coefficients ranges from 0.7 (θp) to 0.95 (Hs). The BIAS is generally low; however, the Hybrid Statistical Downscaling method provides larger BIAS for the Hs and performs better (lower BIAS) for both Tp and θp. Finally, scatter indexes are below 0.4.

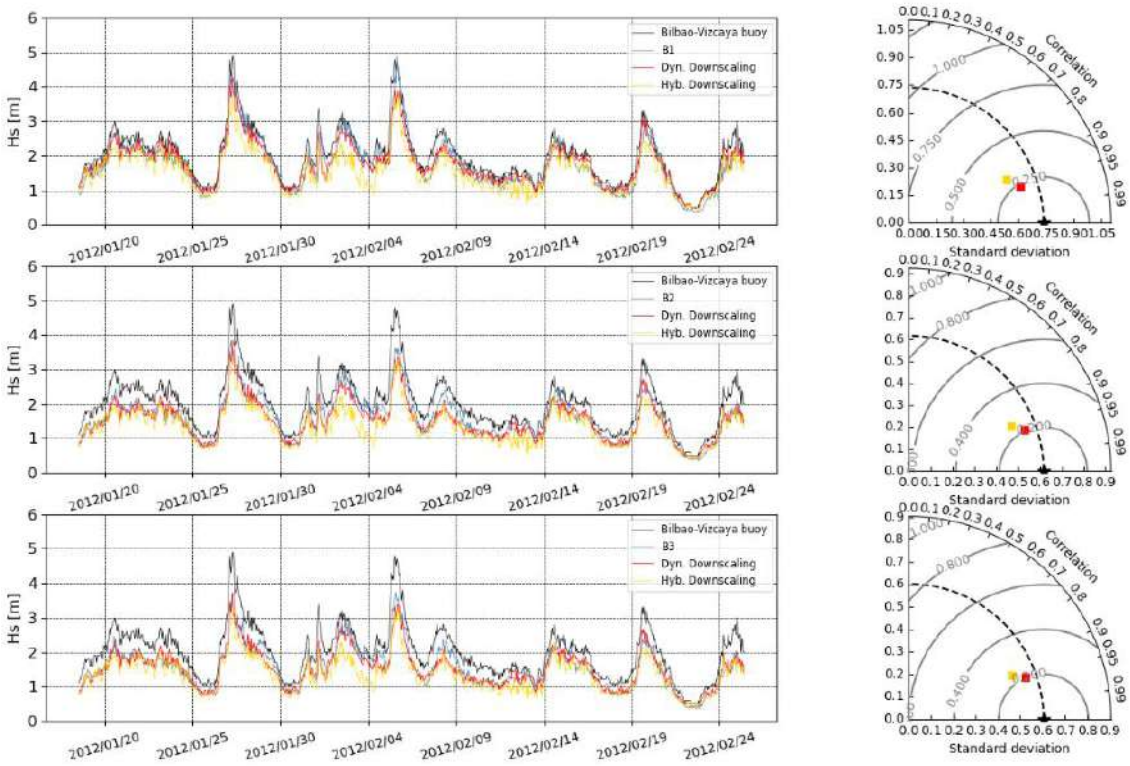

Figure 4 - Downscaling methodology performance at the B1, B2 and B3 control points.

5. Aguçadora (Portugal)

The Aguçadoura test site, situated in the northern region of Portugal (Figure 5), is exposed to the North Atlantic wave regime. The test site, covering an area of about 3.0 km^2, is located approximately 5.5 km offshore with water depths ranging between 40 and 50 meters. The nearest monitoring station is the Leixões coastal buoy, anchored at a depth of 83 meters, and operated by the Instituto Hidrográfico. Data collected by the Leixões buoy from 2018 to February 2023 has been used to characterize the wave climate. The recorded data generally indicates that the main wave direction is from West to North-northwest, with significant wave height values ranging from 1.0 to 5.0 meters. In the case of extreme storm events, significant wave heights can reach up to 10.0 meters. A more detailed analysis of the wave climate can be found in section 3.2.

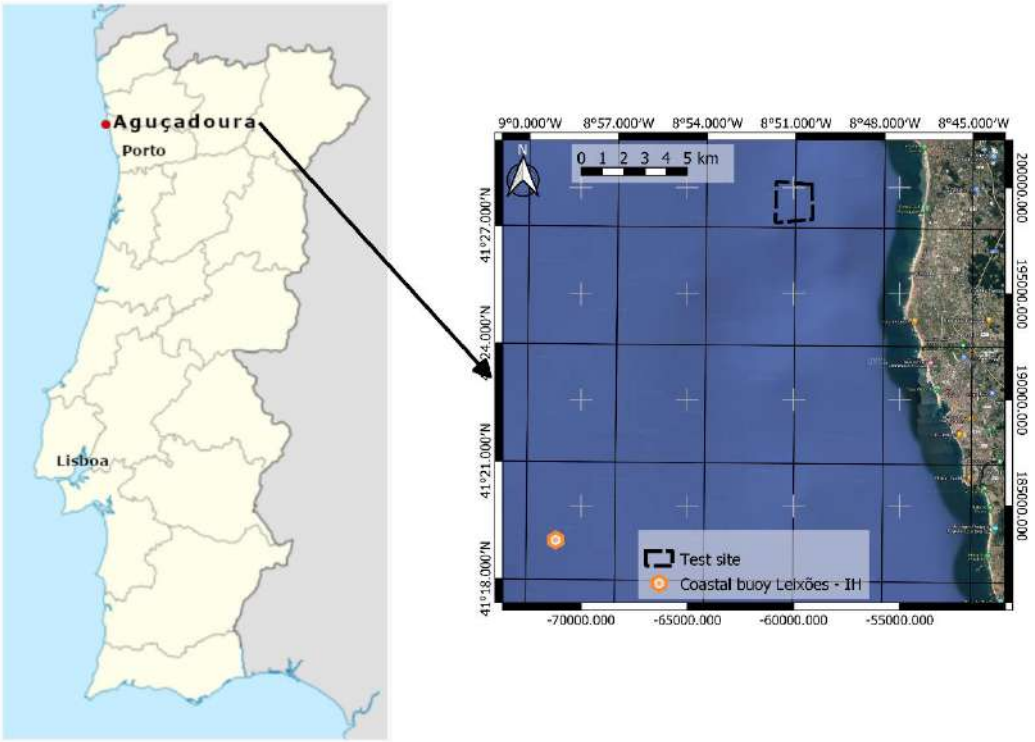

Figure 5 - Aguçadoura test site.

5.1 Simulating WAves Nearshore (SWAN) and SNL-SWAN

The SWAN wave model, a third-generation wave model developed at Delft University of Technology, computes random, short-crested wind-generated waves in coastal regions and inland waters (Booij et al., 1999). Among other factors, SWAN accounts for the following physical processes:

- Wave propagation in time and space, wave shoaling, refraction.
- Wave generation by wind.
- Whitecapping, bottom friction and depth-induced breaking.
- The SWAN wave model can produce the main integral parameters as well as 2D wave spectrum.

The SNL-SWAN model (Ruehl et al., 2013) introduces a modification by adding a WEC module to enhance the way SWAN accounts for the power performance of WECs and their effects on the wave field. This modified version of SWAN uses obstacles to represent WECs. Changes were made on how the transmission coefficient is calculated and five different "obcase" setting options are available. The WEC information can be inputted as a power matrix (POWER.TXT file, Figure 6), and for a power matrix populated with values aggregated over real sea waves, the OBCASE=1 setting is more appropriate. Obstacle case 1 employs the WEC power matrix to determine the effective transmission coefficient and a constant value for this coefficient is applied across all frequencies.

		Tp														
	MEAN	3	4	5	6	7	8	9	10	11	12	13	14	15	16	17
Hs (m)	0.5	4.44	5.07	7.97	12.15	16.77	17.14	11.94	9.16	6.57	4.39	4.00	3.00	2.86	1.95	1.71
	1	16.65	19.00	29.48	46.94	56.61	52.38	37.14	28.73	19.84	16.62	12.94	9.33	7.29	7.40	4.49
	1.5	0.00	41.54	63.14	92.37	110.74	109.49	64.96	55.91	38.49	29.09	22.06	19.26	12.74	11.21	11.50
	2	0.00	66.29	99.03	150.67	200.97	164.91	105.27	85.30	58.63	52.31	40.56	28.76	24.22	19.31	17.57
	2.5	0.00	0.00	160.23	241.82	261.83	226.36	166.20	117.65	83.09	69.87	57.47	39.24	28.51	26.20	23.73
	3	0.00	0.00	212.52	319.26	372.09	327.17	210.96	151.98	116.43	93.66	75.42	66.09	44.81	42.09	30.83
	3.5	0.00	0.00	270.15	436.02	503.15	407.75	292.71	208.22	148.33	115.49	92.63	74.81	57.97	44.27	41.16
	4	0.00	0.00	0.00	553.82	540.26	521.33	355.46	260.73	191.66	144.19	122.78	84.04	81.01	55.80	53.24
	4.5	0.00	0.00	0.00	645.46	746.22	586.83	378.72	302.18	236.42	189.64	154.41	105.88	89.58	74.26	55.78
	5	0.00	0.00	0.00	796.15	926.13	694.67	485.91	341.08	287.07	211.41	167.83	135.72	111.21	93.81	77.53
	5.5	0.00	0.00	0.00	989.38	954.73	807.95	603.12	429.61	343.03	231.19	201.49	150.14	120.29	96.75	89.90
	6	0.00	0.00	0.00	0.00	1161.42	956.67	642.03	480.81	329.09	289.47	212.26	171.77	145.82	110.89	100.85
	6.5	0.00	0.00	0.00	0.00	1476.47	1039.27	702.04	487.62	396.60	311.56	236.66	203.88	153.43	120.26	102.25
	7	0.00	0.00	0.00	0.00	1664.93	1197.05	820.77	612.40	465.98	384.59	251.62	222.70	180.55	146.28	131.44
	7.5	0.00	0.00	0.00	0.00	1608.45	1407.61	922.63	708.98	508.65	373.47	325.45	229.49	190.53	151.78	149.26

Figure 6 – Sample of a WEC power matrix (https://snl-waterpower.github.io/SNL-SWAN/application.html).

Another important aspect of WEC simulation is the calculation of the action density flux between neighbouring grid points. SWAN first determines if the connecting grid line crosses an obstacle line. If, and only if, a grid line is crossed by an obstacle line, the transmission coefficient is applied to the flux between those nodes. Figure 7 provides examples of how to implement obstacles in SNL-SWAN. The red line demonstrates the proper use of obstacle implementation. The two blue obstacles in the figure have the exact same influence on the model solution. The green obstacle, which does not intersect any computational grid lines, will have no effect on the wave propagation.

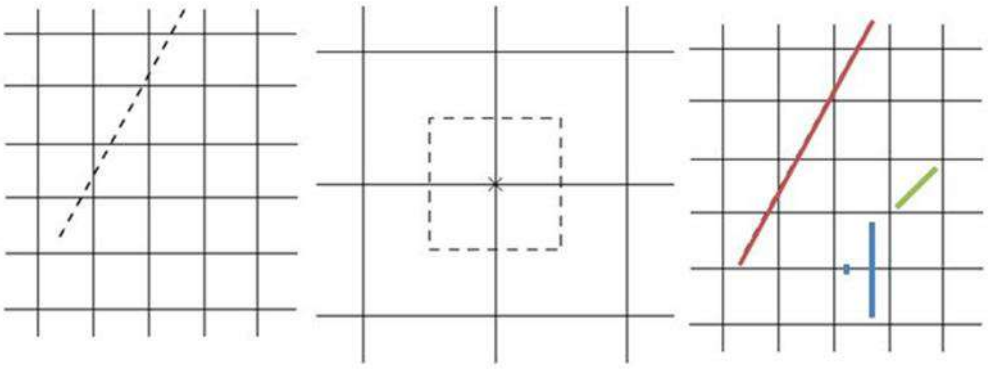

Figure 7 – Obstacle lines cutting through a computational grid.

5.1.1 CorPower Wave Energy Converter

The equipment being simulated at the Aguçadoura test site is the HiWave-5 (Figure 8) from CorPower. The HiWave-5 project involves the final phase of research and testing to implement a new sustainable methodology for electricity production using high-performance Wave Energy Converters (WECs). The project aims to demonstrate a fully integrated WEC system at a commercial scale through dry and ocean testing in Stage 4, followed by an ocean demonstration of a pilot array consisting of three devices in Stage 5.

An essential information for simulating this WEC unit is the power matrix provided by CorPower (Figure 9). The power matrix represents CorPower Ocean's target for energy production by 2030. It is expressed in terms of sea-state parameters, such as significant wave height and energy period, and is the result of computer simulations.

The simulations performed to generate the power matrix, according to CorPower; only include conversion chain losses (e.g., downtime, array interaction losses, electrical farm losses, and auxiliary consumption) for each wave energy converter (WEC) unit, and do not account for external system losses. The total system efficiency term for each WEC is approximately $\eta_{sys} \approx 0.865$.

Figure 8 – HiWave-5 WEC unit.

			Tp (s)																		
			2.8	3.9	5.0	6.1	7.2	8.3	9.4	10.6	11.7	12.8	13.9	15.0	16.1	17.2	18.3	19.4	20.6	21.7	22.8	23.9
			Te [s]																			
			2.5	3.5	4.5	5.5	6.5	7.5	8.5	9.5	10.5	11.5	12.5	13.5	14.5	15.5	16.5	17.5	18.5	19.5	20.5	21.5
			2 3	3 4	4 5	5 6	6 7	7 8	8 9	9 10	10 11	11 12	12 13	13 14	14 15	15 16	16 17	17 18	18 19	19 20	20 21	21 22
	0.25	0	0.5	0.2	0.7	1.4	2.3	3.5	4.6	5.8	6.7	7.7	9.1	9.9	11.2	12.2	13.2	13.7	14.8	15.5	16.0	16.0	16.4
	0.75	0.5	1	2.0	5.7	11.7	19.3	28.2	36.1	42.7	48.3	55.1	61.1	64.7	71.9	72.9	74.4	78.3	76.6	79.0	77.4	78.0	77.3
	1.25	1	1.5	5.6	15.8	31.7	49.8	71.1	89.2	106.3	118.7	130.0	140.4	148.4	150.2	152.9	153.5	151.9	152.2	151.3	147.8	143.7	137.2
	1.75	1.5	2	10.7	30.0	60.3	96.6	132.0	167.3	186.6	212.0	225.9	236.8	243.9	242.9	243.5	241.0	236.5	228.0	223.7	215.4	212.0	203.9
	2.25	2	2.5	17.5	48.1	97.6	155.8	207.9	254.9	295.9	316.4	331.5	333.3	340.2	337.8	336.2	329.8	327.9	310.4	296.1	291.2	287.8	271.2
	2.75	2.5	3	0.0	72.9	142.9	223.9	298.6	359.9	398.4	400.0	400.0	400.0	400.0	400.0	400.0	400.0	400.0	394.3	383.6	373.0	347.5	336.1
	3.25	3	3.5	0.0	98.2	195.7	306.2	400.0	400.0	400.0	400.0	400.0	400.0	400.0	400.0	400.0	400.0	400.0	400.0	400.0	400.0	400.0	400.0
	3.75	3.5	4	0.0	0.0	254.4	389.9	400.0	400.0	400.0	400.0	400.0	400.0	400.0	400.0	400.0	400.0	400.0	400.0	400.0	400.0	400.0	400.0
	4.25	4	4.5	0.0	0.0	320.1	400.0	400.0	400.0	400.0	400.0	400.0	400.0	400.0	400.0	400.0	400.0	400.0	400.0	400.0	400.0	400.0	360.0
	4.75	4.5	5	0.0	0.0	0.0	400.0	400.0	400.0	400.0	400.0	400.0	400.0	400.0	400.0	400.0	400.0	400.0	400.0	400.0	400.0	400.0	320.0
	5.25	5	5.5	0.0	0.0	0.0	400.0	400.0	400.0	400.0	400.0	400.0	400.0	400.0	400.0	400.0	400.0	400.0	400.0	400.0	400.0	400.0	280.0
	5.75	5.5	6	0.0	0.0	0.0	400.0	400.0	400.0	400.0	400.0	400.0	400.0	400.0	400.0	400.0	400.0	400.0	400.0	400.0	400.0	360.0	240.0
	6.25	6	6.5	0.0	0.0	0.0	0.0	400.0	400.0	400.0	400.0	400.0	400.0	400.0	400.0	400.0	400.0	400.0	400.0	400.0	400.0	320.0	200.0
	6.75	6.5	7	0.0	0.0	0.0	0.0	400.0	400.0	400.0	400.0	400.0	400.0	400.0	400.0	400.0	400.0	400.0	400.0	400.0	400.0	280.0	160.0
Hs [m]	7.25	7	7.5	0.0	0.0	0.0	0.0	400.0	400.0	400.0	400.0	400.0	400.0	400.0	400.0	400.0	400.0	400.0	400.0	400.0	400.0	240.0	120.0
	7.75	7.5	8	0.0	0.0	0.0	0.0	360.0	360.0	360.0	360.0	360.0	360.0	360.0	360.0	360.0	360.0	360.0	360.0	360.0	360.0	200.0	80.0
	8.25	8	8.5	0.0	0.0	0.0	0.0	320.0	320.0	320.0	320.0	320.0	320.0	320.0	320.0	320.0	320.0	320.0	320.0	320.0	320.0	160.0	40.0
	8.75	8.5	9	0.0	0.0	0.0	0.0	280.0	280.0	280.0	280.0	280.0	280.0	280.0	280.0	280.0	280.0	280.0	280.0	280.0	280.0	120.0	0.0
	9.25	9	9.5	0.0	0.0	0.0	0.0	240.0	240.0	240.0	240.0	240.0	240.0	240.0	240.0	240.0	240.0	240.0	240.0	240.0	240.0	80.0	0.0
	9.75	9.5	10	0.0	0.0	0.0	0.0	200.0	200.0	200.0	200.0	200.0	200.0	200.0	200.0	200.0	200.0	200.0	200.0	200.0	200.0	40.0	0.0
	10.25	10	10.5	0.0	0.0	0.0	0.0	160.0	160.0	160.0	160.0	160.0	160.0	160.0	160.0	160.0	160.0	160.0	160.0	160.0	160.0	0.0	0.0
	10.75	10.5	11	0.0	0.0	0.0	0.0	120.0	120.0	120.0	120.0	120.0	120.0	120.0	120.0	120.0	120.0	120.0	120.0	120.0	120.0	0.0	0.0
	11.25	11	11.5	0.0	0.0	0.0	0.0	80.0	80.0	80.0	80.0	80.0	80.0	80.0	80.0	80.0	80.0	80.0	80.0	80.0	80.0	0.0	0.0
	11.75	11.5	12	0.0	0.0	0.0	0.0	40.0	40.0	40.0	40.0	40.0	40.0	40.0	40.0	40.0	40.0	40.0	40.0	40.0	40.0	0.0	0.0
	12.25	12	12.5	0.0	0.0	0.0	0.0	0.0	0.0	0.0	0.0	0.0	0.0	0.0	0.0	0.0	0.0	0.0	0.0	0.0	0.0	0.0	0.0
	12.75	12.5	13	0.0	0.0	0.0	0.0	0.0	0.0	0.0	0.0	0.0	0.0	0.0	0.0	0.0	0.0	0.0	0.0	0.0	0.0	0.0	0.0
	13.25	13	13.5	0.0	0.0	0.0	0.0	0.0	0.0	0.0	0.0	0.0	0.0	0.0	0.0	0.0	0.0	0.0	0.0	0.0	0.0	0.0	0.0
	13.75	13.5	14	0.0	0.0	0.0	0.0	0.0	0.0	0.0	0.0	0.0	0.0	0.0	0.0	0.0	0.0	0.0	0.0	0.0	0.0	0.0	0.0
	14.25	14	14.5	0.0	0.0	0.0	0.0	0.0	0.0	0.0	0.0	0.0	0.0	0.0	0.0	0.0	0.0	0.0	0.0	0.0	0.0	0.0	0.0
	14.75	14.5	15	0.0	0.0	0.0	0.0	0.0	0.0	0.0	0.0	0.0	0.0	0.0	0.0	0.0	0.0	0.0	0.0	0.0	0.0	0.0	0.0

Figure 9 – HiWave-5 power matrix (supplied by CorPower in the framework of the project).

5.2 Local wave climate

The wave climate at Aguçadoura is primarily influenced by waves generated in the North Atlantic. An analysis of the data collected by the Leixões buoy over the last 5 years, from 2018 to February 2023, reveals that the main incident wave direction is from West to North-northwest, accounting for 91.47% of the registered data. The most frequent significant wave heights from this sector range from 0.5 to 5.0 m (Figure 10). However, during severe storms, significant wave heights can reach up to 10.0 m. Waves from the West to South-southwest sector represent 5.89% of the records, with the most frequent significant wave heights ranging from 0.5 to 4 m. The maximum wave height registered in this period is 15.6 m from West.

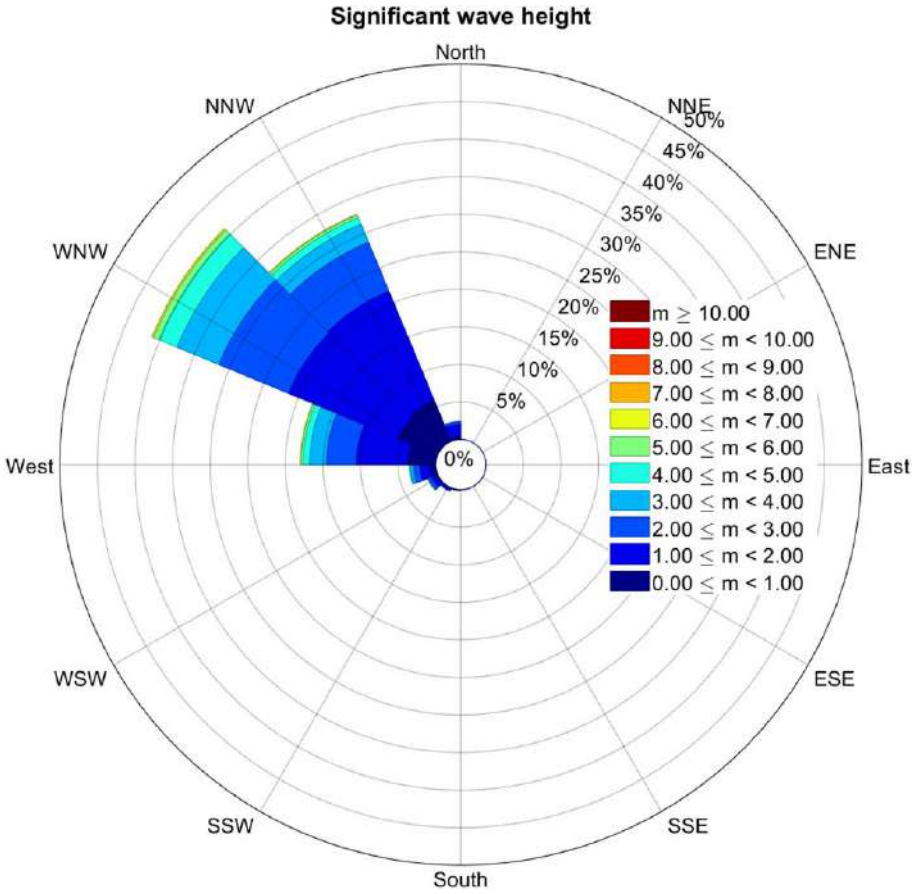

Figure 10 – Significant wave height distribution by incoming direction.

The peak periods are predominantly concentrated between 8 to 16 s (86.51%), associated with significant wave heights from 0.5 to 4.0 m (Figure 11). Higher peak periods have also been recorded, but they account for only 1.59% of the data.

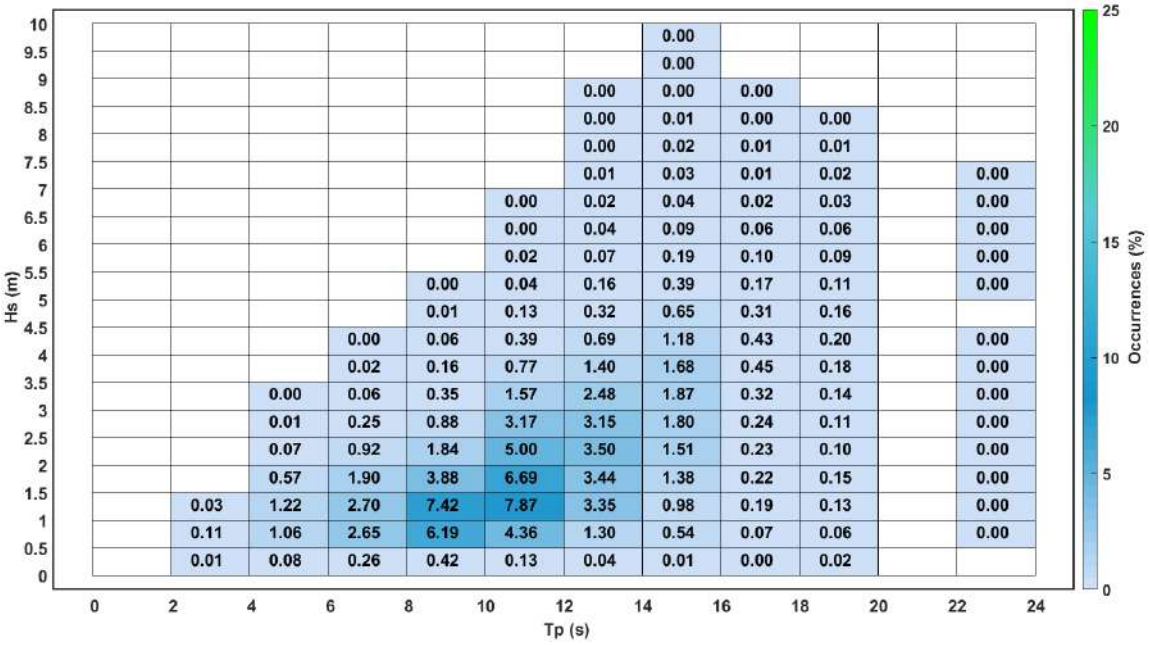

Figure 11 – Significant wave height distribution by peak period.

5.3 WEC farm modelling

The primary objective of the present work is to evaluate the influence of the WEC farm on nearshore coastal processes, such as sediment transport, at the Aguçadoura test site. To achieve this, a series of modelling steps are required. In this section, the relevant steps taken to model the WEC farm and the results obtained are presented.

5.3.1 WEC farm

The WEC farm being modelled consists of four groups of seven HiWave-5 WEC units each (Figure 12), capable of producing approximately 10 MW. It has a North-South length of 2210 m, an East-West width of 150 m, and each WEC unit is spaced 150 m apart from one another.

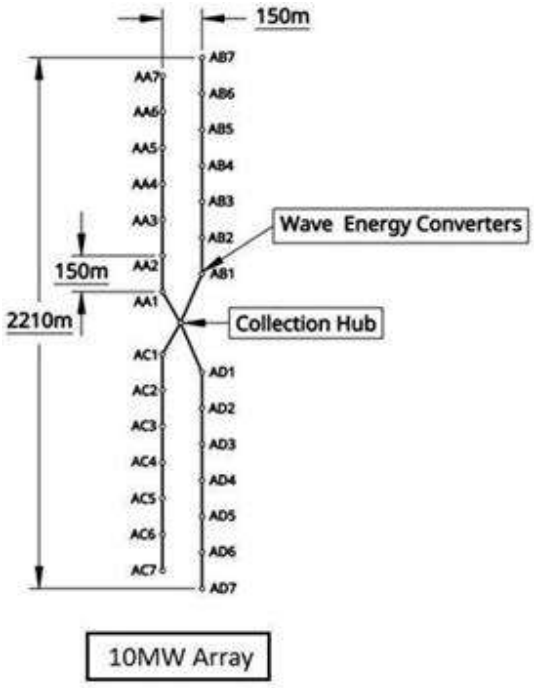

Figure 12 – WEC farm implemented.

5.3.2 Modelling domain

The modelling domain for the simulation must be in accordance with the size of the WEC farm and consider the potential affected area due to the shadowing effect of the farm. Furthermore, the grid resolution must be fine enough to properly represent the dimensions of the WEC units. In Figure 13, the generated modelling domain can be seen. The spatial coverage is much larger, measuring 8.5 km cross-shore and 7.7 km along-shore, compared to the area occupied by the WEC farm. To simulate the HiWave-5 point absorber unit, a resolution of at least 9.0 m is required.

The definition of the WEC shape and grid resolution considers the best practices previously mentioned for the SNL-SWAN. An initial set of simulations were conducted using various grid resolutions and WEC shapes. The tested grid resolutions were 9.0, 4.5, and 3.0 m, and the WEC shapes consisted of a single straight line, an L shape, and a square shape. The results achieved with the higher grid resolutions, 4.5 and 3.0 m, were very time-consuming. Additionally, testing the various shapes of the WEC unit, such as L and square shapes, can lead to inconsistent results in terms of power absorption, usually resulting in values exceeding the WEC's capability.

The adopted configuration for the WEC unit is a single straight line that intersects one computational grid line, with a grid resolution of 9.0 m.

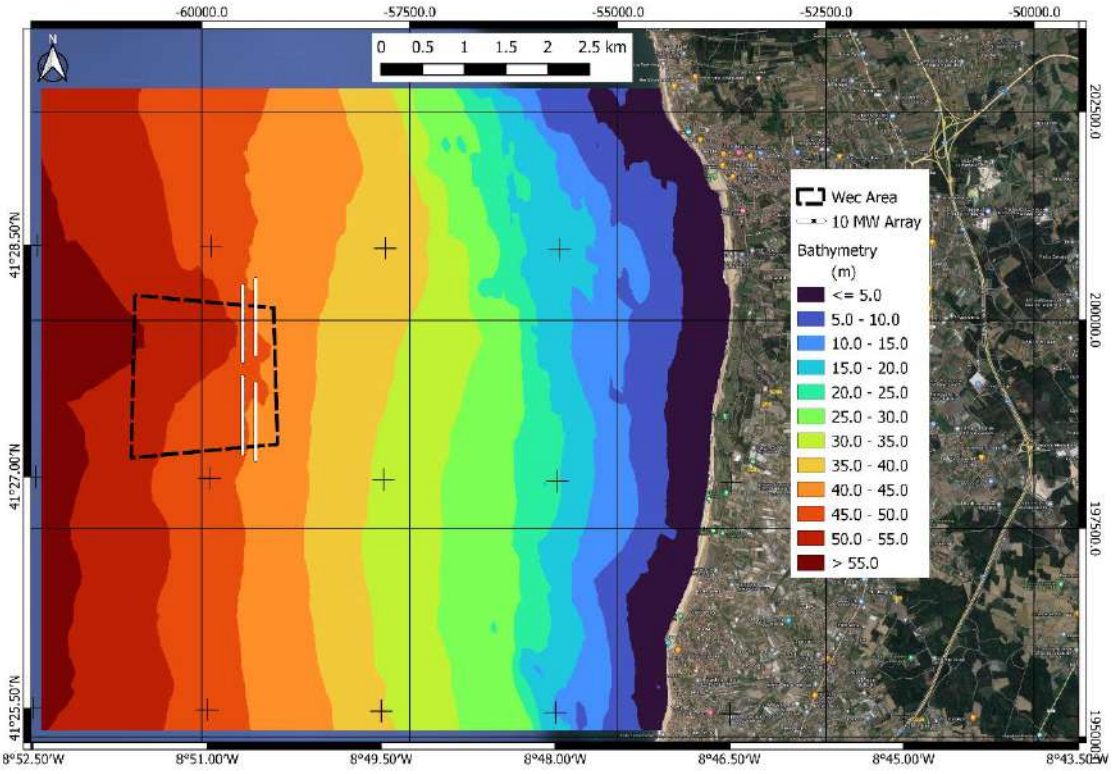

Figure 13 – Modelling domain.

5.3.3 Boundary conditions

The boundary conditions used for the wave model have a 15-day range and consider typical high-energy events for the Portuguese coast. From the data collected by the Leixões buoy (Figure 14) , it is possible to see that there are four high-energy events (2022/10/15 to 2022/10/25) with significant wave heights above 4.0 m, peak periods ranging from 6 to 15 s, and covering an incoming sector from 200° to 330°. After October 25 (see Figure 14) less energetic wave conditions occur with significant wave heights between 1.0 to 3.0 m, peak periods from 6.0 to 15.0 s, and incoming waves from 220° to 315°.

The implementation of these sea states in the wave model is done in the form of wave spectral energy information. As mentioned earlier, this information comes from the Portuguese operational wave model that is described in Annex A.

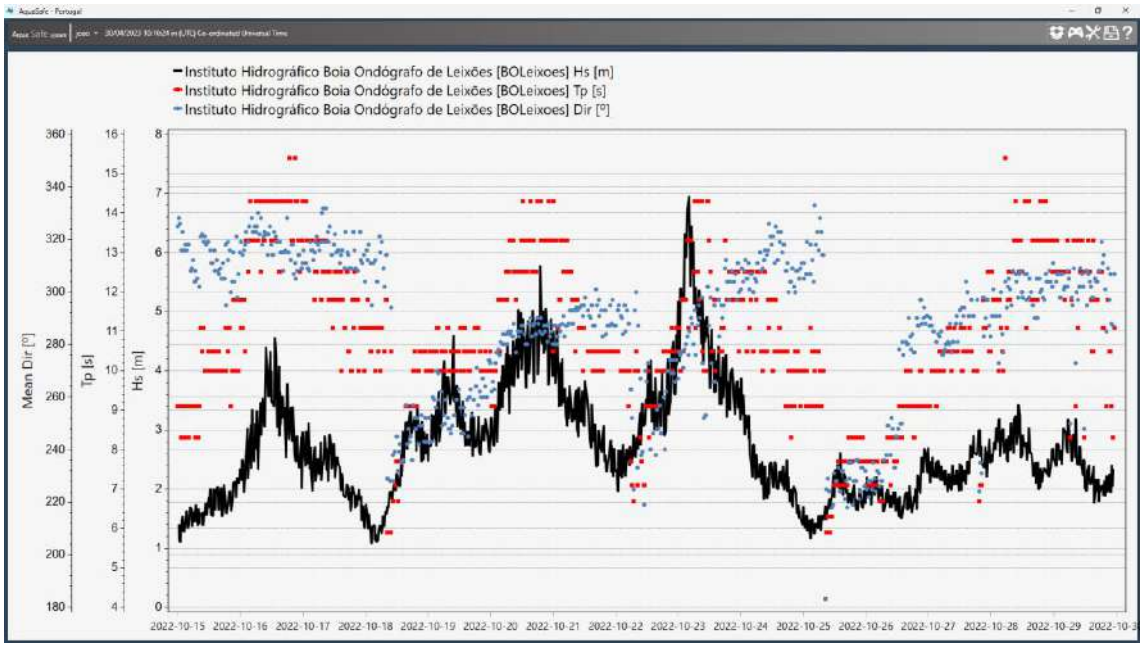

Figure 14 – Collected data from the Leixões buoy.

5.3.4 WEC farm simulation results

In this section, the results from the WEC farm simulation are presented. Considering just one WEC unit, there is a 68% reduction in energy at the lee of the equipment over the 15-day period (Table 2). Additionally, the wave power timeseries illustrates the influence of the WEC unit in its vicinity (Figure 15).

The incoming wave power is represented in Figure 15 by "Incident-Wp", while "Lee-WP represents the integration of wave power in several grid cells to the lee of the WEC unit and "Incident-Lee" represents the difference between the two. This shows how the SWAN-SNL is handling wave power removed by the WEC unit.

The results presented here are obtained from a real sea wave spectrum (wind generated wave spectrum). This can explain the difference between "Incident-Lee" and "WECMatrix-Wp" and lead to an expected 20% reduction in energy production calculated by the numerical model.

The whole WEC farm production forecast can be determined by calculating the difference between the energy flux of the WEC and NoWEC scenarios. This is done by extracting a profile immediately to the East along the WEC arrays closest to shore. In the scenario without a WEC farm, the accumulated energy flux along this profile, over the 15-day period, ranges between 14.35 MWh/m and 15.84 MWh/m. However, in

the scenario with the WEC farm, the accumulated energy flux along the same profile, for the same time interval, ranges between 6.78 MWh/m and 15.67 MWh/m (Figure 16). Integrating booth profiles over the mesh size and calculating the difference between them, a value of 2620.12 MWh is obtained (Figure 16).

Table 2 – 15 days energy reduction.

15 Days time integration (1 WEC)	
Incident (kw.h)	139580.7
Lee (kW.h)	44886.6
Change(%)	-68%

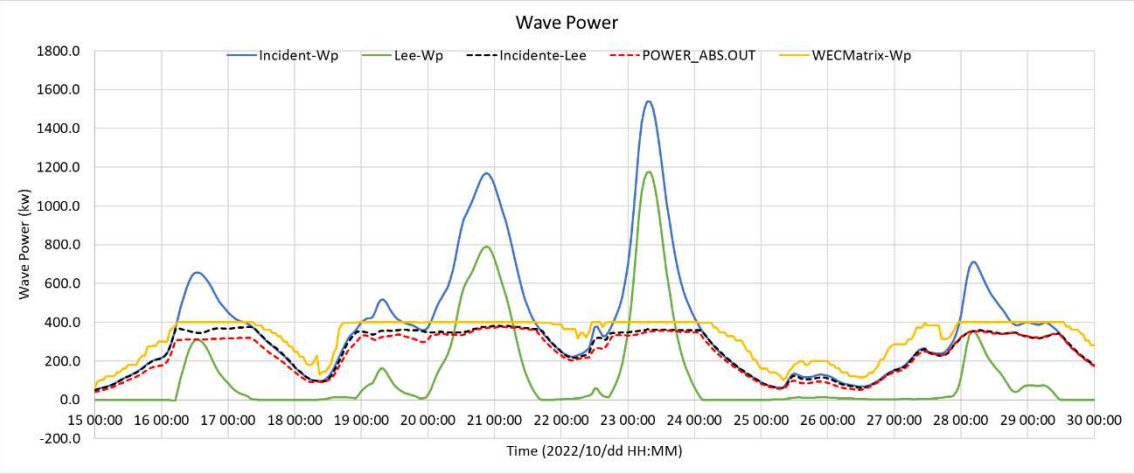

Figure 15 – Wave power time series for one WEC unit.

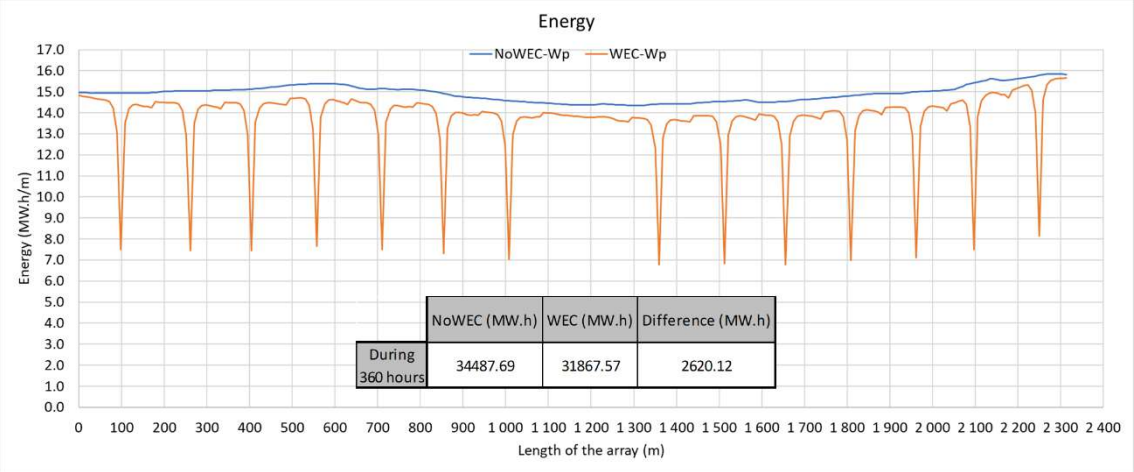

Figure 16 – Energy flux profile for the WEC and no WEC situation and forecasted production.

The purpose of this section is not to evaluate the efficiency of the WEC unit or the energy production of the WEC farm, but to understand possible differences arising from numerical or configuration errors. The results presented here are obtained from a real sea wave spectrum boundary condition, rather than the JONSWAP wave spectrum. This distinction can lead to variations in power absorption results compared to the expected wave power matrix. Additionally, the WEC configuration and the method used to solve the transmission coefficient can introduce further uncertainties. However, it is possible to calculate a relation coefficient of 1.2 by performing a linear regression analysis on the 'incident-lee' power timeseries and the WEC matrix power timeseries.

When comparing to the theoretical production capacity of the farm, 11.2 MW (400kW times 28 WEC units) for a 15-day period (4032 MWh), this corresponds to a 65% production efficiency for the farm during this period (Table 3). It is essential to keep in mind that the 11.2 MW value is without any energy losses and the 10MW farm includes conversion chain losses as mentioned above in the 5.1.1 section.

Table 3 – 15 days energy production estimation.

	Energy Production (MW.h)		
	Model	11.2MW Array	Estimated production
During 360 hours (15 days)	2620.12	4032.00	65%

5.3.4.1 WEC influence range

In this section, the range of influence of the WEC farm is analysed. This is achieved through the integration of the energy flux data from a 15-day simulation run, in two separate scenarios: one that includes the WEC farm, and another without it. The results of these simulations are visualized in Figure 17 and Figure 18 respectively.

Observing these maps, a decrease in energy flux is visible in the scenario involving the WEC farm. The most significant changes in energy flux patterns occur up to the -55000 easterly grid line (approximately 4.3 km to lee of the farm).

The energy flux patterns in the nearshore regions, on both maps, are found to be nearly identical (beyond the -55000 easterly grid line). This suggests that the influence of the WEC farm on the coastal area is minimal. Despite the presence of the WEC farm and

the ensuing decrease in energy flux, this does not appear to significantly impact the wave energy flux arriving at the coast.

This observation is important because it indicates that while WEC farms can influence the wave propagation, their impact on the nearshore waves (a critical factor in coastal ecosystems and processes such as sediment transport and beach erosion) is not significant.

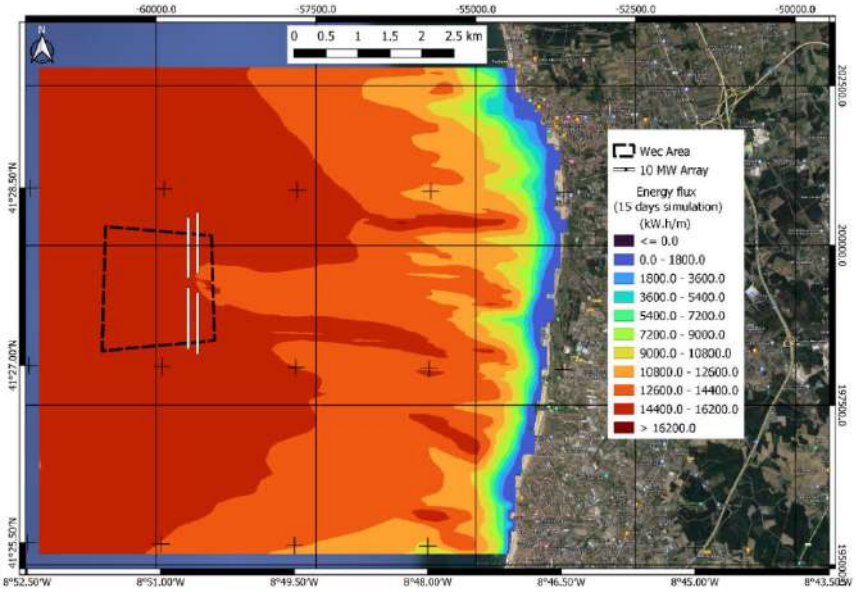

Figure 17 – Accumulated 15-day wave energy flux distribution without WEC farm.

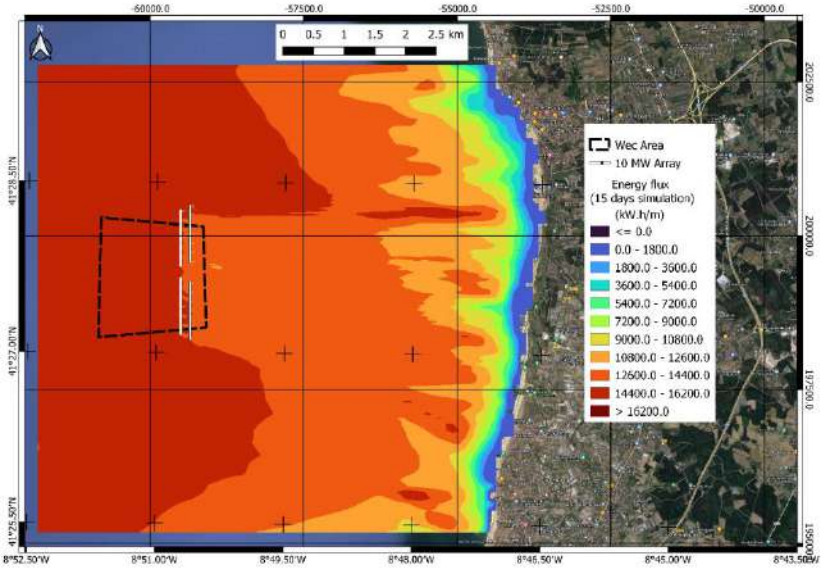

Figure 18 – Accumulated 15-day wave energy flux distribution in presence of WEC farm.

To better understand and quantify the WEC farm's influence nearshore, maps of wave energy differences have been produced (Figure 19). The most significant reduction occurs immediately to the lee of the WEC farm, exceeding 1900.0 kW.h/m. Closer to the shore, the reduction in wave energy progressively diminishes, with values lower than 200 kW.h/m.

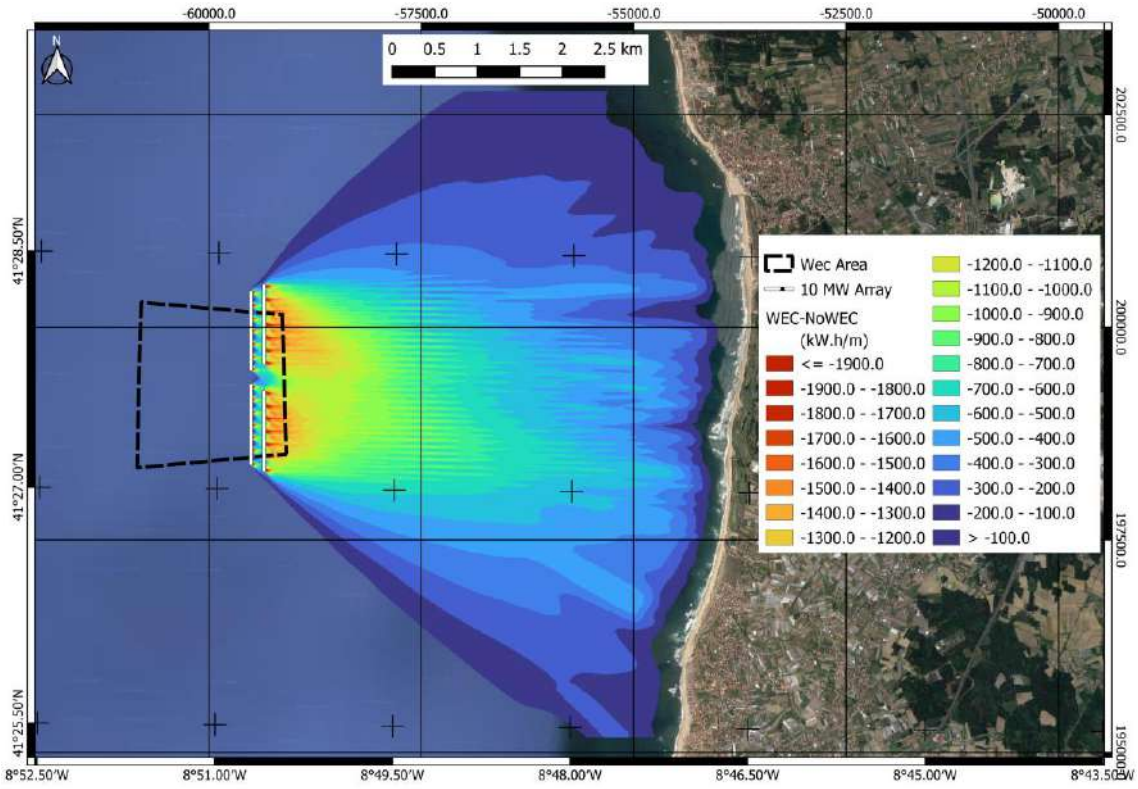

Figure 19 – Wave energy reduction due to the presence of the WEC farm.

A more effective way to visualize the WEC farm's influence is in terms of percentage. As shown in Figure 20 , the reduction near the WEC farm is above 10%, while closer to the shore, it ranges between 4% and 1%. By zooming in on the WEC farm (Figure 21), it is evident that reductions above 45% can occur immediately to the lee of each WEC unit.

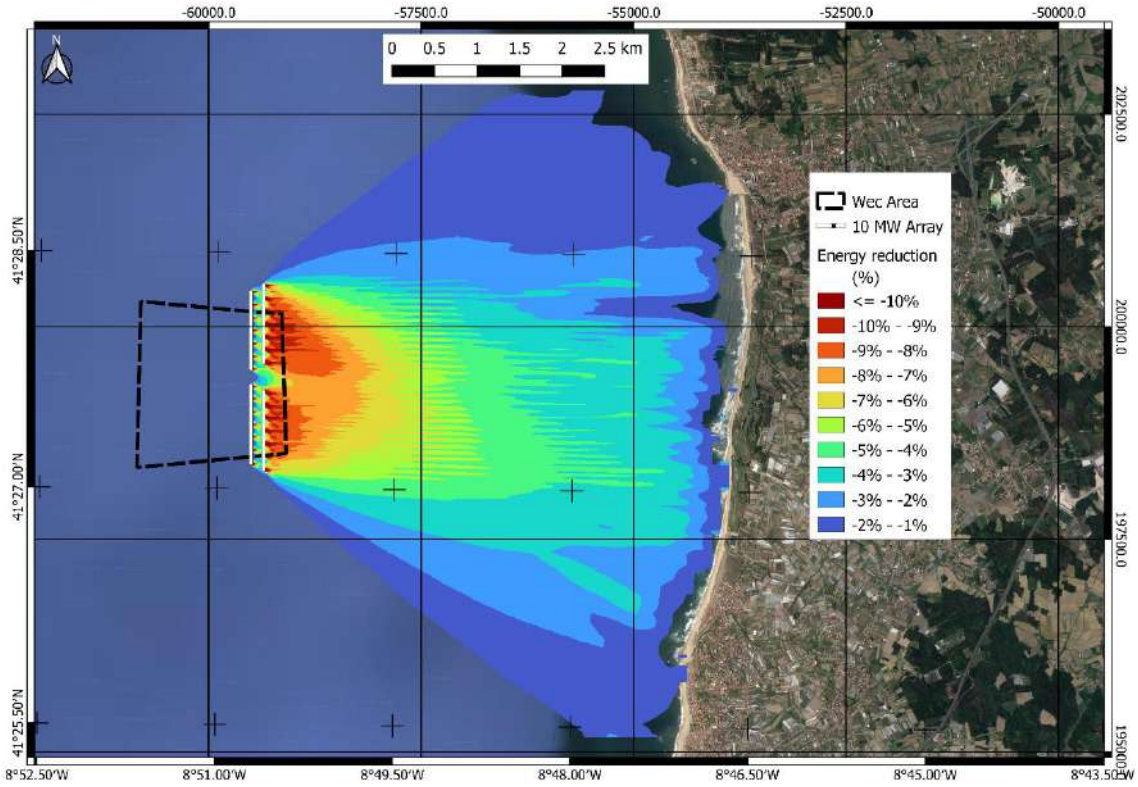

Figure 20 – Percentual energy reduction due to the presence of the WEC farm.

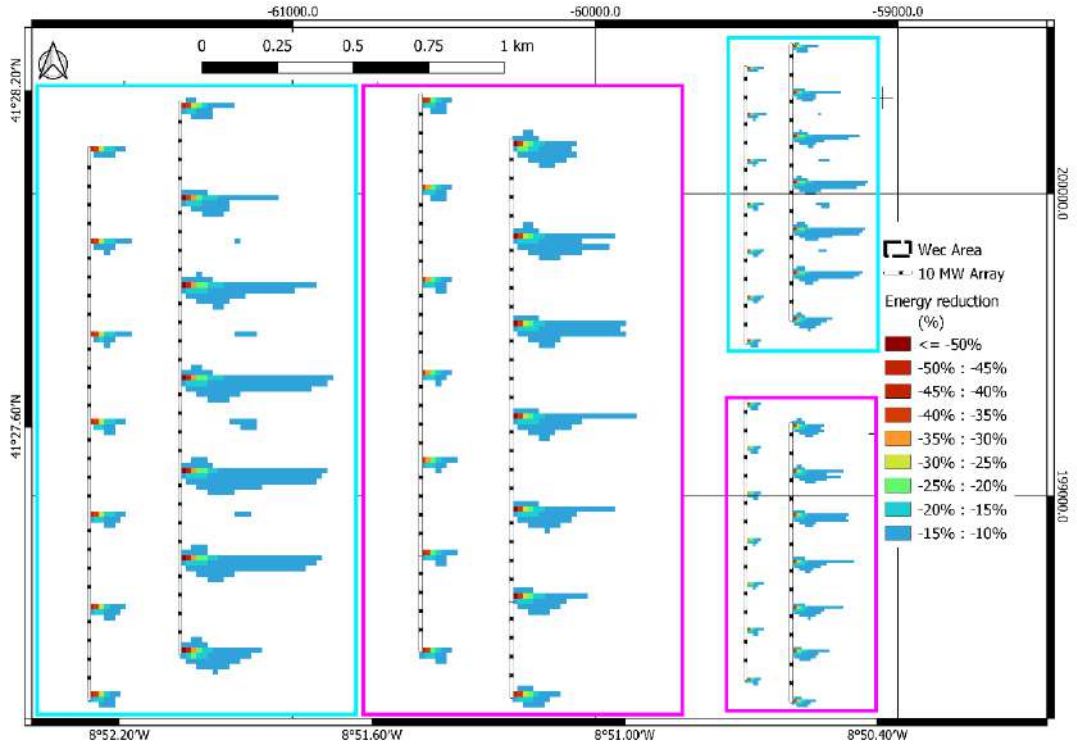

Figure 21 – Percentual energy reduction due to the presence of the WEC farm. WEC units zoom.

Additionally, timeseries perpendicular to the coast were extracted (Figure 22). This information will help understand how the influence of the WEC farm affects the nearshore area. Out of eight virtual monitoring stations, four are presented. Monitoring station A serves as a control point, allowing the validation of the imposed wave boundary conditions, ensuring that they are correct and in line with the data collected by the Leixões buoy. Monitoring station C is where the influence of the WEC farm is most felt (monitoring station B is too close to the gap between arrays, and the reduction there is negligible). Monitoring stations G (1200 m offshore at 10 m depth) and H (300 m offshore at 2 m depth) will provide information on how the waves are reaching the shore. Both are more than 4.5 km away from the WEC farm.

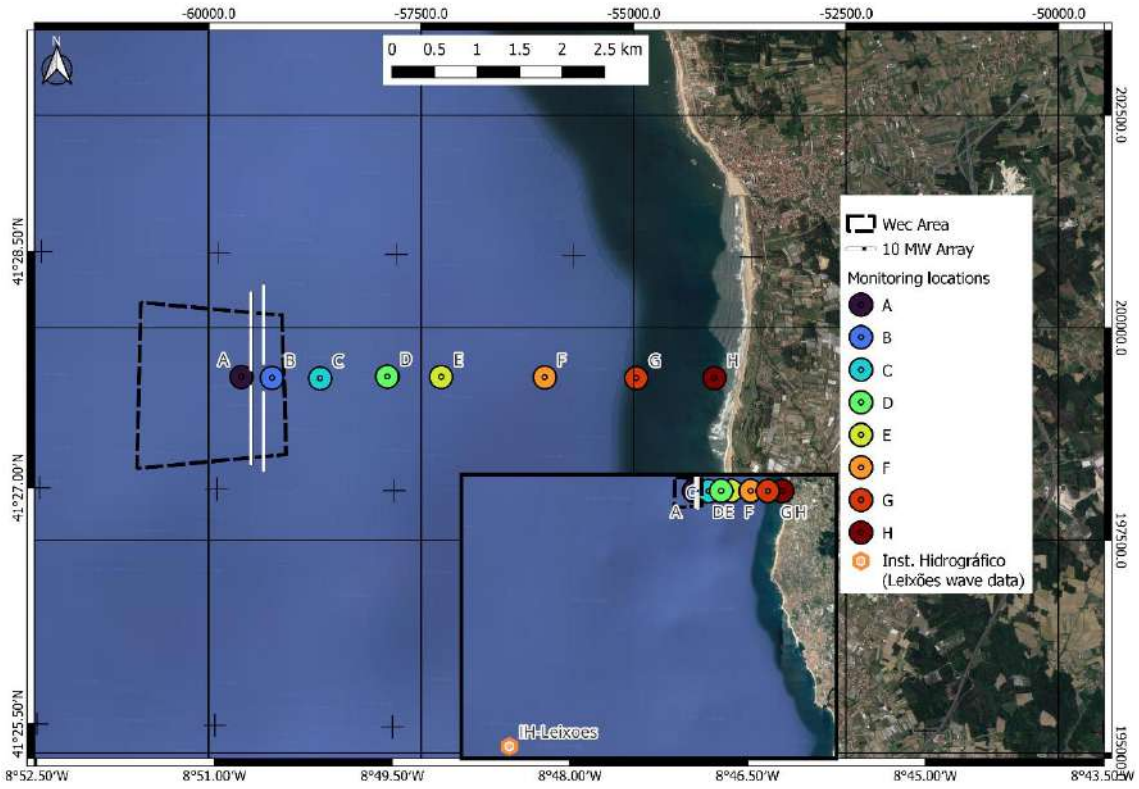

Figure 22 – Timeseries location.

From monitoring station A (Figure 23), it is evident that the significant wave height values are in accordance with the data recorded by the Leixões buoy, meaning that the imposed boundary conditions are correct. Also, there is no change in the wave power, as expected.

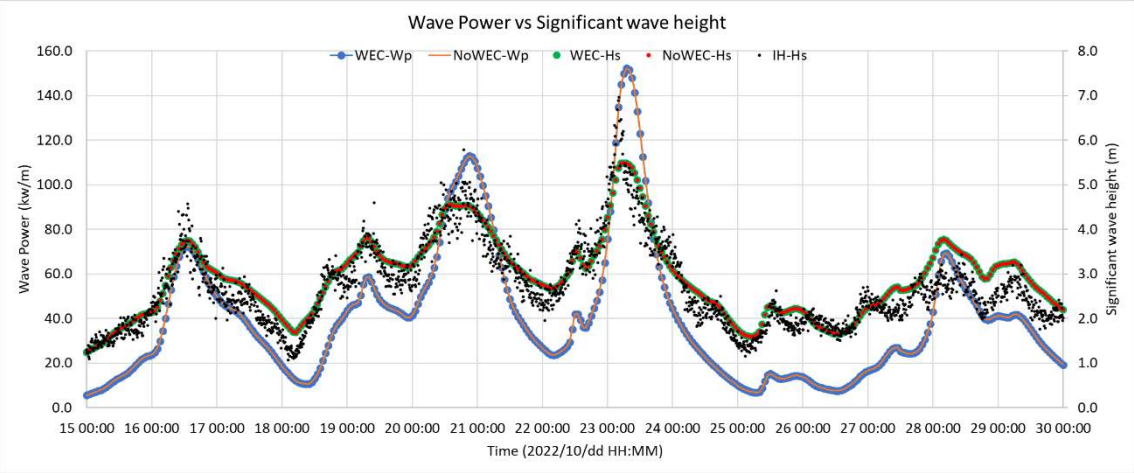

Figure 23 – Timeseries at monitoring station A. Comparison between the significant wave height and wave power incident to the wave farm.

The timeseries at monitoring station C demonstrates the influence of the WEC farm (Figure 24). At this location, a reduction in both significant wave height and wave power can be observed. Although minimal, on the order of centimetres, the significant wave height with the presence of the WEC farm (yellow dots) is smaller than the situation without the WEC farm (black dots). The wave power for the two scenarios shows a clear difference.

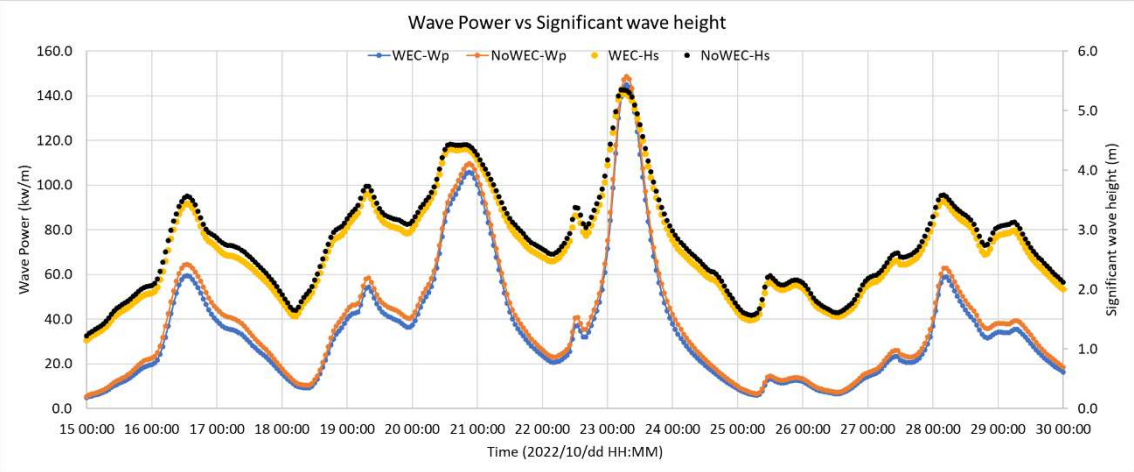

Figure 24 – Timeseries at monitoring station C. Comparison between the significant wave height and wave power to the lee of the wave farm.

Analysing the two selected nearshore monitoring locations, G and H (Figure 25, Figure 26), it is evident that there is no influence from the WEC farm. At both locations, the significant wave height shows no difference, and the same can be said for the wave power. In Annex A, additional time series of wave peak period and mean wave direction are represented. Again, no relevant change occurs between the scenarios with and without the WEC farm, for the nearshore locations.

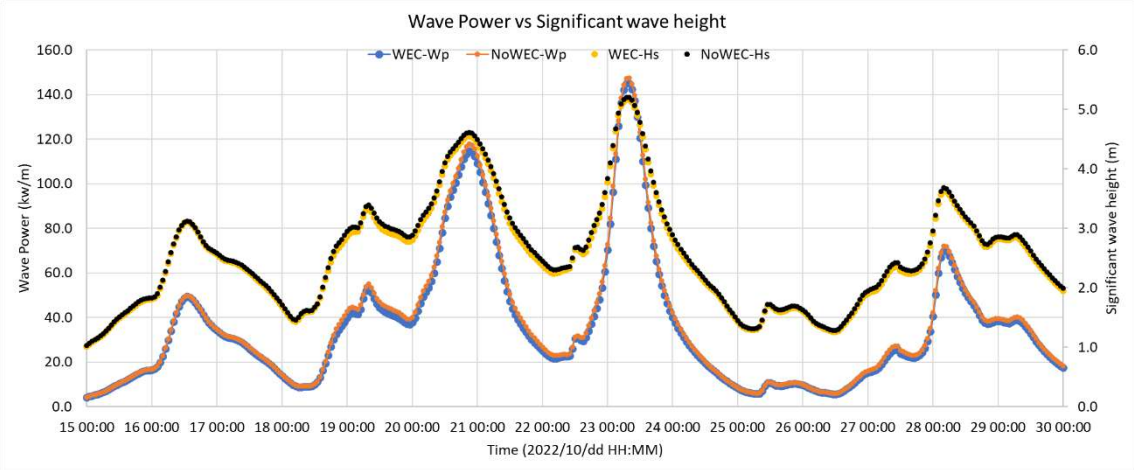

Figure 25 – Timeseries at monitoring station G. Comparison between the significant wave height and wave power to the lee of the wave farm.

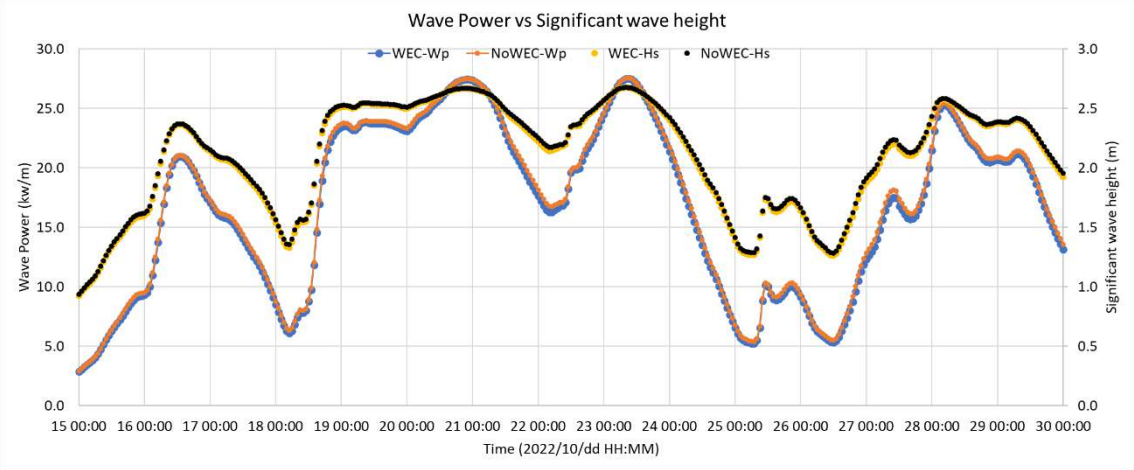

Figure 26 – Timeseries at monitoring station H. Comparison between the significant wave height and wave power to the lee of the wave farm.

6. Conclusions

6.1 BIMEP

In the present study, the validation of the Hybrid Statistical Downscaling methodology followed in (de Santiago, I., Moura, T., Chambel, J., Liria, P., and Bald, 2020) within the WESE project (https://wese-project.weebly.com/) is carried out. For that, '*in situ*' wave parameter measures are compared with modelled at three different locations within the BIMEP area.

The model grid cell size sensitivity test shows that there is a clear relationship between the grid cell size and the computational cost. However, the grid cell sizes tested in the present work have a limited impact on the output. In general, larger grid configuration has larger errors however, maximum RMSE values of 0.5 m, 0.4 s and 2° for Hs, Tp and θp, respectively are found. This indicates that the model used is robust and stable.

The comparison between Downscaling methods reveals the suitability of Hybrid Statistical Downscaling approach to be carried out in probabilistic wave farm coastal impact studies. The differences between the use of Dynamic Downscaling and Hybrid Statistical Downscaling are small and acceptable for this type of work (RMSE is below 0.28m, 1.52s and 13.14° for Hs, Tp and θp). Hybrid Statistical Downscaling method provides larger BIAS for the Hs than Dynamic Downscaling but performs better (lower BIAS) for both Tp and θp.

6.2 Aguçadoura

For the Aguçadoura test site in Portugal, the simulation of one WEC unit demonstrates how the SNL-SWAN model interacts with the WEC device and what energy extraction is expected. In this case, there is a 68% reduction in energy to the lee of the equipment over a 15-day period.

The simulation results of the WEC farm reveals that the most considerable energy reduction takes place right to the lee of the site, with a reduction exceeding 10% and a maximum extension of 250.0 m. The shadowing effect gradually diminishes towards the shore, with the reduction nearshore being less than 2%.

Virtual monitoring stations were defined to provide a better understanding of the WEC farm's influence. Monitoring station C clearly displays the impact of the WEC farm,

with reductions in significant wave height and wave power. Monitoring stations G and H are more than 4.5 km away from the WEC farm, with energy reduction ranging from 4% to 1%. The timeseries at these two locations indicates that changes in wave power are two orders of magnitude lower than the incident wave power in the shoreline. By analysing the mean wave direction timeseries (Annex A) it becomes evident that monitoring station C exhibits slight variations in direction. The changes observed are minimal from WNW and become more pronounced when shifting towards WSW. Contrarywise, no discernible alterations in wave direction are observed for the two monitoring stations, G and H, located closest to the shore. This observation holds significance as changes in wave direction near shore can have a direct impact on sediment transport.

The results achieved with these simulations indicate that a WEC farm located at the Aguçadoura site would not influence the sediment transport at the shore or any other processes.

Finally, it is essential to consider the computational effort needed to simulate the WEC farm. To accurately assess the extent of the wave farm's influence, large computational domains are required. Additionally, the computational grid must have a resolution capable of simulating the WEC unit. These two factors make the simulation effort very time-consuming and for these reasons other approaches should be tested. The options may vary from using other models similar to SNL-SWAN, or even adopting a statistical downscaling approach following the methodology described for the BIMEP case. In any case, this may not be a straightforward task. At the Aguçadoura test site, a wave spectrum generated by wind is used (real wave spectrum). The BIMEP test site uses a method based on a characterization of sea states from wave integral parameters, then, a JONSWAP theoretical formulation is applied to simulate the wave propagation. It would be relevant to evaluate the difference between these two modelling parametrizations, particularly in terms of how they influence the WEC energy production and the wave propagation near the shore.

7. BIBLIOGRAPHY

Booij, N.R.R.C., Ris, R.C., Holthuijsen, L.H., 1999. A third-generation wave model for coastal regions: 1. Model description and validation. J. Geophys. Res. Ocean. 104, 7649–7666.

Camus, P., Mendez, F.J., Medina, R., 2011. A hybrid efficient method to downscale wave climate to coastal areas. Coast. Eng. 58, 851–862.

Camus, P., Mendez, F.J., Medina, R., Tomas, A., Izaguirre, C., 2013. High resolution downscaled ocean waves (DOW) reanalysis in coastal areas. Coast. Eng. 72, 56–68. https://doi.org/10.1016/j.coastaleng.2012.09.002

Chang, G., Ruehl, K., Jones, C.A., Roberts, J., Chartrand, C., 2016. Numerical modeling of the effects of wave energy converter characteristics on nearshore wave conditions. Renew. Energy 89, 636–648.

de Santiago, I., Moura, T., Chambel, J., Liria, P., and Bald, J., 2020. Deliverable 3.3 Marine dynamics modelling. Deliverable of the WESE Project funded by the European Commission. Agreement number EASME/EMFF/2017/1.2.1.1/02/SI2.787640.

Ruehl, K., Porter, A., Posner, A., and Roberts, J., 2013. Development of SNL-SWAN, a Validated Wave Energy Converter Array Modeling Tool. Proceedings of the 10th European Wave and Tidal Energy Conference.

CorPower Ocean's. 2023. HiWave-5 power matrix www.corpowerocean.com/powermatrix/PM22003_CPO_target_2030

8. Annex A

This section contains a description of Hidromod's wave forecasting operational system and includes additional results from the virtual monitoring stations previously mentioned in the document.

8.1.1 Portuguese operacional wave model

The operational wave forecasting system for the Portuguese coast was developed during the Advanced Meteo-Oceanographic Forecasting Services for the Sea (AMOS) project, which took place from 2015 to 2016. Within the framework of AMOS, an operational forecasting system was established, covering Portugal's mainland and the Azores and Madeira archipelagos, based on the AQUASAFE platform. To produce the required forecasts, the models were properly implemented and underwent a validation procedure.

8.1.1.1 Forecasting methodology

The operational system employs a downscaling methodology, implementing successive higher resolution domains focused on specific regions. This system can be divided into two stages. The first stage is run at a global scale, starting with a domain that covers the entire globe with a 1-degree resolution in longitude and latitude. This level provides boundary conditions for the next nested level, the North Atlantic Ocean.

The second level, the North Atlantic Ocean model, has a spatial resolution of a quarter degree and supplies wave spectrum boundary conditions to three coastal regional models: the Portuguese mainland, the Azores islands, and the Madeira islands. This stage is simulated using the WaveWatch 3 wave model, with GFS winds driving the wave generation.

The second stage consists of the above-mentioned regional models with 0.01-degree resolution, covering the Portuguese mainland, Azores, and Madeira. These models already provide valuable offshore forecasting information and play an important role in the wave modelling system, as they allow for downscaling to high-resolution models by supplying the required boundary conditions. This stage is simulated using the SWAN wave model, with high-resolution local winds used for forcing locally generated waves.

8.1.1.2 Validation (Leixões)

The validation process is a crucial aspect as it allows the evaluation of the model's performance. Although the validation of the operational wave modelling system is an ongoing procedure and a continuous improvement process, the initial validation was carried out for the year 2014. Table 4 presents the results of the validation, and generally, the wave model demonstrates a good agreement with the observed data.

Table 4 - Validation table for the Portuguese mainland's coastal area.

Parameter	Station	BIAS	RMSE	R
Significant wave height	Leixões	0.28 m	0.55 m	0.96
	Sines	0.30 m	0.50 m	0.96
	Faro	-0.08 m	0.24 m	0.93
Peak wave period	Leixões	-2.55 s	3.10 s	0.80
	Sines	-2.16 s	2.64 s	0.85
	Faro	-1.18 s	2.90 s	0.59
Wave direction	Leixões	-7.44 º	18.58 º	0.71
	Sines	-4.85 º	12.29 º	0.73
	Faro	10.94 º	33.48 º	0.79

8.1.2 Virtual monitoring stations results

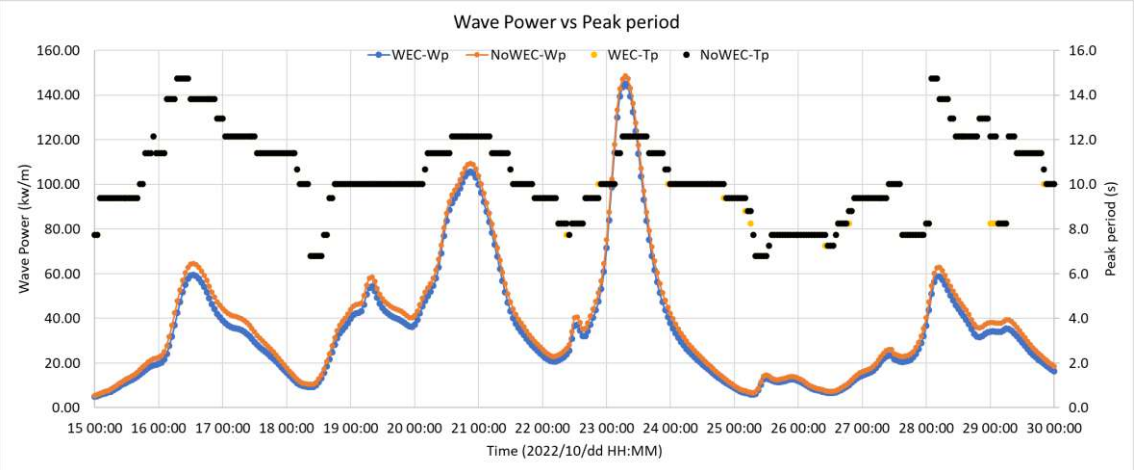

Figure 27 – Timeseries at monitoring station C. Comparison between the peak period and wave power lee to the wave farm.

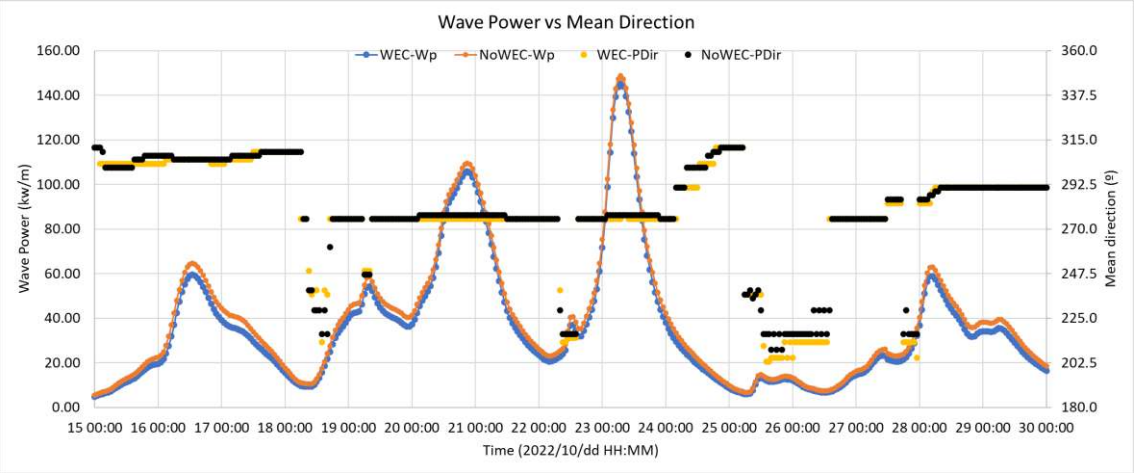

Figure 28 – Timeseries at monitoring station C. Comparison between the mean wave direction and wave power lee to the wave farm.

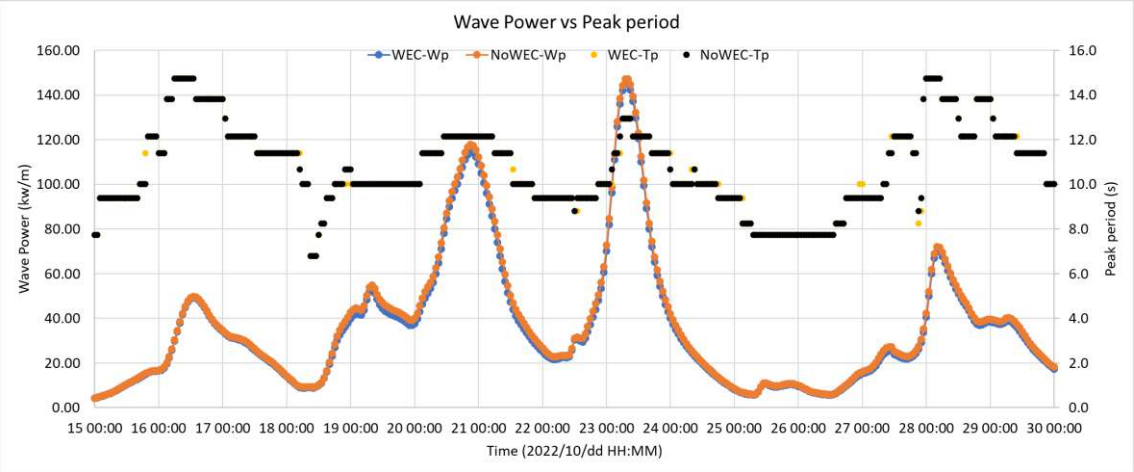

Figure 29 – Timeseries at monitoring station G. Comparison between the peak period and wave power lee to the wave farm.

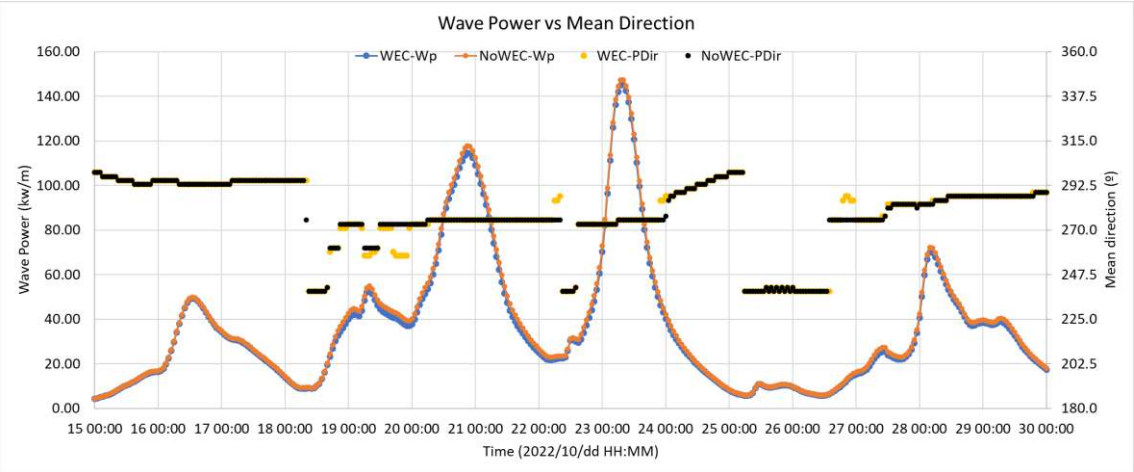

Figure 30 – Timeseries at monitoring station G. Comparison between the mean wave direction and wave power lee to the wave farm.

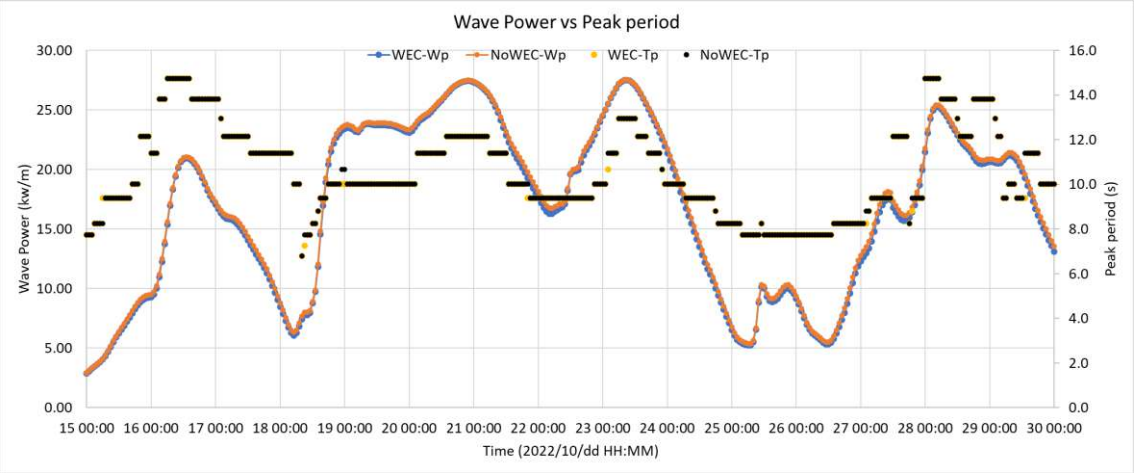

Figure 31 – Timeseries at monitoring station H. Comparison between the peak period and wave power lee to the wave farm.

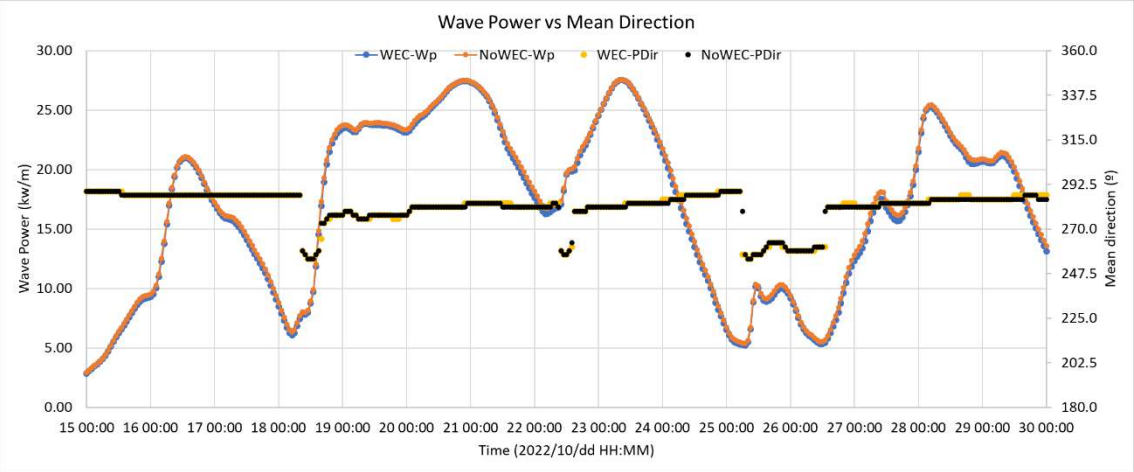

Figure 32 – Timeseries at monitoring station H. Comparison between the mean wave direction and wave power lee to the wave farm.